

Scanning electrochemical microscopy

Kinetics of chemical reactions following electron-transfer measured with the substrate-generation–tip-collection mode

Rachel D. Martin and Patrick. R. Unwin†

Department of Chemistry, University of Warwick, Coventry, UK CV4 7AL

The substrate-generation–tip-collection (SG–TC) mode of the scanning electrochemical microscope (SECM) is used as a new approach to investigate the kinetics of EC processes. Under the conditions of interest, a species O is generated at a macroscopic substrate (generator) electrode, with potential-step control, through the diffusion-limited electrolysis of a solution species R (E step). As O diffuses away from the generator, it undergoes a first order chemical reaction in solution (C step). A fraction of O is collected by electrolysis back to R at an externally biased ultramicroelectrode (UME), positioned directly over the substrate. This promotes the diffusional feedback of R to the substrate. Theory for the problem, relating the time-dependent tip current response to the rate constant for the C step and the tip–substrate electrode separation is developed numerically. Results of the calculations illustrate how the characteristic features of the tip current transients: peak current, peak time and post-half-peak time, depend on the kinetics of the C step and the inter-electrode separation. It is shown that both the kinetics and tip–substrate separation can be determined independently from a single transient by simply measuring the peak current and peak time. The theoretical results are validated experimentally through model studies of the oxidative deamination of *N,N*-dimethyl-*p*-phenylenediamine (DMPPD) in aqueous solution at high pH. The effective second-order rate constant for the deamination step is in excellent agreement with values measured by alternative methods.

In addition to the well documented use of SECM^{1,2} as a probe of interfacial kinetics,³ a number of papers have demonstrated that SECM is a powerful device for measuring the solution kinetics of chemically unstable electrogenerated species.^{4–6} Processes studied by SECM include chemical reactions following electron transfer, such as first order EC^{4,7} and second-order EC_{2i}^{5,8,9} mechanisms, and chemical reactions sandwiched between two one-electron transfer steps as in the ECE-DISP1 framework.⁶

The investigation of electrode processes involving coupled homogeneous kinetics with SECM has largely been based on the feedback mode,^{2,4–9} or closely related tip-generation–substrate-collection (TG–SC) mode.^{5,6,8–10} With these approaches, the tip UME, positioned directly over a larger collector electrode, is held at a potential to electrogenerate the species of interest from a solution precursor at a diffusion-controlled rate. A competition is then established between the diffusion of the electrogenerated species to the collector electrode, maintained at a potential to promote the regeneration and feedback of the initial precursor, and the solution kinetics. By measuring the tip feedback current or tip and substrate currents as a function of tip–substrate separation (which governs the inter-electrode diffusion time), the kinetics of the solution process can be determined with high precision over a wide dynamic range.^{4–9}

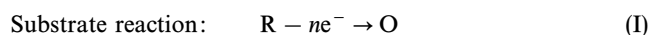
These approaches require that the separation between the tip and substrate is well defined and variable. This parameter can be obtained by ensuring that the two electrodes are aligned with sufficient precision that they can be approached to contact, and then withdrawn a known distance (the method employed for the studies in this paper). Alternatively, the tip–substrate separation can be obtained by measurement of the solution resistance,¹¹ although this approach has not been widely used. The most common method for determining the inter-electrode separation (employed for all studies of homogeneous kinetics hitherto), is to use an internal mediator as a calibrant of the tip–substrate separation, but there are

instances where this may interfere with the reaction of interest.⁸

The SG–TC mode is an alternative, but less used, approach for investigating homogeneous kinetics.^{12–14} This mode was introduced by Engstrom and co-workers^{12,13} in a configuration where an amperometric tip UME served to collect both stable and transient species generated at a larger electrode. In these studies, a semi-quantitative theoretical model for the collector electrode response was developed, with the neglect of feedback effects, and used to estimate the kinetics of the follow-up chemical reaction.¹³

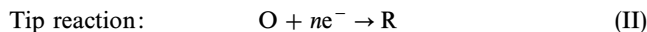
It has been suggested that theoretical modelling of the SG–TC mode with amperometric electrodes would prove difficult because of feedback effects and the complex interaction of the diffusion layers on the two electrodes.^{3a} However, we have recently demonstrated that, for a simple redox couple, the tip UME response can readily be described taking account of these processes.¹⁵ In combination with feedback measurements,¹⁶ the SG–TC mode was shown to be a simple, but powerful, approach for identifying subtle differences in the diffusion coefficients of the reduced and oxidised forms of a redox couple, without prior knowledge of the sizes of the electrodes or their separation.^{15,16} In this paper we extend the SG–TC model to electrode processes involving irreversible following chemical reactions, of the first-order EC type, and demonstrate that the transient response of the tip UME allows the solution kinetics and inter-electrode separation to be determined independently, negating the need for a distance calibrant or sophisticated positioning apparatus for this type of SECM measurement.

Under the conditions of interest, the SG–TC mode involves the diffusion-controlled electrogeneration of a species, *e.g.* O, at a macroscopic substrate electrode from a solution species, *e.g.* R.

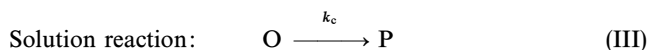


Species O diffuses away from the substrate and is intercepted by a tip (collector) UME, where it undergoes diffusion-controlled reduction back to R.

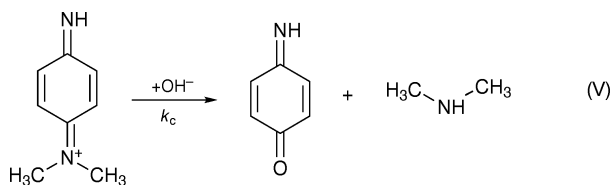
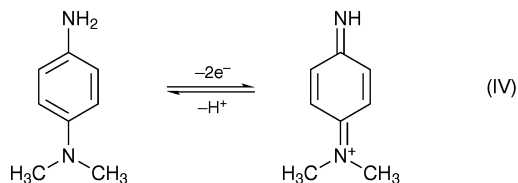
† E-mail: P.R.Unwin@warwick.ac.uk



During transport from the substrate to the tip, O may also decompose in a first-order irreversible chemical process, with a rate constant k_c , to form a product, P, which is electroinactive at the potentials of interest.



A theoretical model for the above processes in the SECM geometry is developed using the alternating direction implicit finite difference method (ADIFDM),^{17,18} which has found widespread application for solving earlier SECM problems.^{4–6,15,16,19–21} The theoretical predictions are verified experimentally with studies on the oxidative deamination of DMPPD in aqueous basic solution, which may be considered as a model EC process.^{4,22–24}



where eqn. (IV) and (V) represent the E step and C step, respectively.

Theory

For the electrode and solution reactions defined by eqn. (I)–(III), the time-dependent diffusion equations for species R and O in the axisymmetric SECM geometry (Fig. 1) are:

$$\frac{\partial c_R}{\partial t} = D_R \left[\frac{\partial^2 c_R}{\partial r^2} + \frac{1}{r} \frac{\partial c_R}{\partial r} + \frac{\partial^2 c_R}{\partial z^2} \right] \quad (1)$$

$$\frac{\partial c_O}{\partial t} = D_O \left[\frac{\partial^2 c_O}{\partial r^2} + \frac{1}{r} \frac{\partial c_O}{\partial r} + \frac{\partial^2 c_O}{\partial z^2} \right] - k_c c_O \quad (2)$$

where r and z are the coordinates in the radial and normal directions starting at the electrode surface, D_i and c_i are the diffusion coefficients and concentrations of species i (R or O), and t is time.

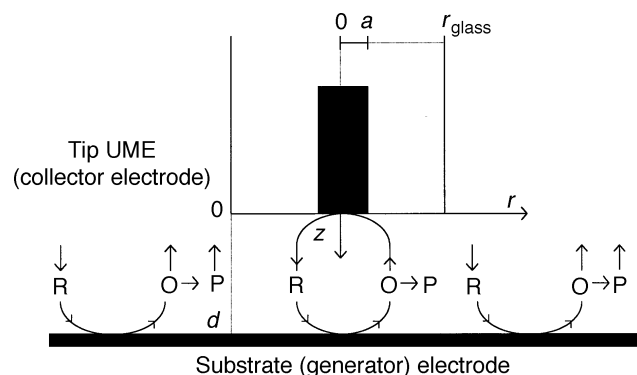


Fig. 1 Schematic diagram of the substrate-generation-tip-collection (SG-TC) mode of SECM for an EC process. The coordinate system for the SECM geometry is also shown. Note that this diagram is not to scale: typically $r_{\text{glass}} \approx 10a$; $d \leq a$.

Initially the solution contains only species R at a bulk concentration, c_R^* , and hence the initial condition within the tip-substrate domain is:

$$0 \leq z \leq d, 0 \leq r \leq r_{\text{glass}}; \quad c_R = c_R^*, c_O = 0 \quad (3)$$

where d is the distance between tip and substrate electrodes and r_{glass} defines the position of the radial edge of the tip.

At time $t = 0$, the potential of the substrate electrode is stepped to a value for the diffusion-controlled oxidation of R [eqn. (I)], while the tip UME is held at a potential to promote the reverse reaction at a diffusion-controlled rate [eqn. (II)]. There is assumed to be no reaction of either R or O on the insulating glass sheath surrounding the tip UME and no radial flux of species at the cylindrical axis of symmetry. Since the UME tip (including the insulating sheath) is smaller than the macroscopic substrate electrode, and $RG = r_{\text{glass}}/a > 10$ for UMEs employed practically and considered theoretically in SECM,^{4–6,15,16,19–21,25} it is reasonable to assume planar diffusion of O and R normal to the substrate electrode at the edge of the tip-substrate domain.¹⁵ The boundary conditions are therefore as follows:

$$z = d, 0 \leq r \leq r_{\text{glass}}; \quad c_R = 0, D_R \frac{\partial c_R}{\partial z} = -D_O \frac{\partial c_O}{\partial z} \quad (4)$$

$$z = 0, 0 \leq r \leq a; \quad c_O = 0, D_O \frac{\partial c_O}{\partial z} = -D_R \frac{\partial c_R}{\partial z} \quad (5)$$

$$z = 0, a \leq r \leq r_{\text{glass}}; \quad D_O \frac{\partial c_O}{\partial z} = D_R \frac{\partial c_R}{\partial z} = 0 \quad (6)$$

$$0 < z < d, r = r_{\text{glass}}; \quad D_O \frac{\partial c_O}{\partial r} = D_R \frac{\partial c_R}{\partial r} = 0 \quad (7)$$

$$0 < z < d, r = 0; \quad D_O \frac{\partial c_O}{\partial r} = D_R \frac{\partial c_R}{\partial r} = 0 \quad (8)$$

The problem was cast into dimensionless form, in order to obtain general solutions, by introducing the following terms:

$$R = r/a \quad (9)$$

$$Z = z/a \quad (10)$$

$$\tau = tD_R/a^2 \quad (11)$$

$$C_i = c_i/c_R^* \quad (i = R \text{ or } O) \quad (12)$$

$$\gamma = D_O/D_R \quad (13)$$

$$K = k_c a^2/D_R \quad (14)$$

Since R is the only electroactive species in bulk solution, it is most convenient to normalise the UME collector current, i_c , for the SG-TC mode¹⁵ with respect to the steady-state current for the oxidation of R at the tip when it is placed at a large distance from the substrate,²⁶

$$i_\infty = 4nFaD_R c_R^* \quad (15)$$

where F is Faraday's constant, to give:

$$i_c/i_\infty = \gamma(\pi/2) \int_0^1 (\partial C_O/\partial Z)_{Z=0} R \partial R \quad (16)$$

It is worth emphasising that this choice of normalisation is necessarily different to that for feedback^{16,25} and other SECM modes,^{19–21} for which the tip reaction is the same in bulk solution and close to the target interface.

The problem was solved numerically using the ADIFDM, for which general details are given elsewhere.^{4–6,15,16,19–21} Programs were written in FORTRAN and run on either the University of Warwick central UNIX system or a local Hewlett-Packard 735 workstation.

Theoretical results and discussion

The normalised current–time response of the tip UME depends primarily on the tip–substrate separation, K and γ . To limit the length of this paper, comprehensive theoretical results are presented for the case of $\gamma = 1$, which both represents the most general case and was appropriate to the experimental system of interest (*vide infra*).

Calculated tip chronoamperometric characteristics for a range of values of the normalised rate constant, at two tip–substrate separations, $\log(d/a) = -0.7$ and -0.2 (typical of relatively small and large separations) are shown in Fig. 2(a) and (b), respectively. In the absence of following chemical reactions ($K = 0$), the tip current rises, after an initial lag period, from zero to a steady-state value. The magnitude of the steady-state current and the rise time depend on the tip–substrate separation, as discussed in detail elsewhere.¹⁵ In brief, the closer the tip and substrate, the shorter the inter-electrode diffusion time. Consequently, in this limiting situation, the more rapid the current rise the sooner a steady state is established. At steady-state, the concentration gradients normal to the UME are steeper the closer the inter-electrode spacing, resulting in an increasingly enhanced current with decreasing electrode separation.

In contrast, for finite values of K , the current does not reach a steady state, rather it rises to a peak value and then decreases at longer times. The value of both K , and the tip–substrate separation, have a marked effect on the overall shape of the tip current transient and the magnitude of the peak current. For a given tip–substrate separation, the larger the value of K , the smaller the peak current, the shorter the time to reach the peak, and the steeper the decay curve following the peak. This is expected, since increasing the rate of the following chemical reaction decreases the fraction of substrate-generated O that initially reaches the tip in the first pass, thereby decreasing the peak current. The extent to which

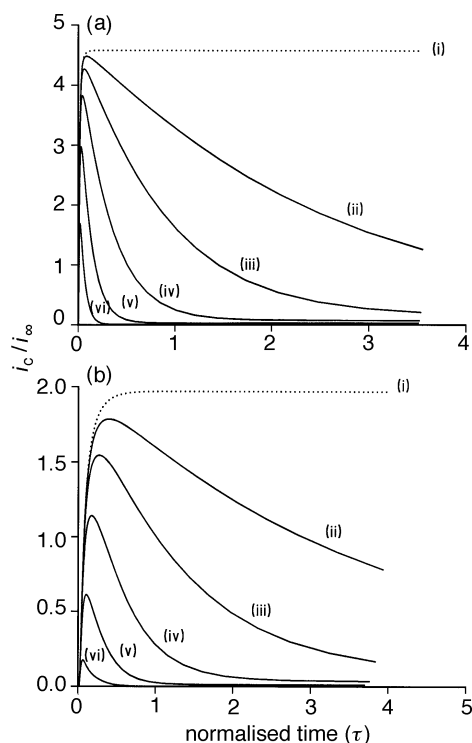


Fig. 2 Effect of K on the chronoamperometric characteristics for an EC process in the SG–TC mode at tip–substrate separations of (a) $\log(d/a) = -0.7$ and (b) $\log(d/a) = -0.2$. Normalised current data are plotted as a function of normalised time, τ . The dashed lines (i) show the behaviour for $K = 0$, while the solid lines are for $\log K$ values of: (ii) -0.5 ; (iii) 0.0 ; (iv) 0.5 ; (v) 1.0 and (vi) 1.5 .

feedback occurs at longer times decreases with increasing rate constant, causing the rapid decay in the current and the appearance of the peak at shorter times.

At the larger tip–substrate separations [Fig. 2(b)] the diffusion time for the substrate-generated species to reach the tip increases. Consequently, for a given value of K , the peak current occurs at a longer time than for the closer tip–substrate separation [Fig. 2(a)]. Moreover, as found for feedback^{2,4–8} and TG–SC^{5,6,8} measurements, the current response becomes less sensitive to solution kinetics, the greater the spacing between the tip and substrate. For the SG–TC mode in the present application, the effect of increasing the inter-electrode spacing is to decrease the peak current for a given value of K . These issues are illustrated further in Fig. 3, which shows transients for $K = 10$ at a range of values of $\log(d/a)$ between -1.0 and -0.5 . It is clear that the closer the tip–substrate separation, the larger the peak current, but the shorter the peak time. From an experimental viewpoint, close tip–substrate separations lead to high sensitivity in terms of tip current, but it is also evident that the tip response has to be measured with the highest temporal resolution in this situation.

The characteristic features of the tip current transients in Fig. 2 and 3 are the peak current, peak time and post-half-peak time. Comprehensive contour plots illustrating how these features depend on the tip–substrate separation and K are given in Fig. 4. The magnitude of the normalised peak current [Fig. 4(a)] increases as both K and the value of d/a are decreased. In contrast, the peak time increases as the value of d/a is increased and K is decreased [Fig. 4(b)]. In principle, this contrasting variation in the peak current and peak time with K and d/a should allow both to be determined from a single transient measurement. The post-half-peak time has a yet different dependence on d/a and K , by increasing as K decreases while showing only a minimal dependence on the inter-electrode separation [Fig. 4(c)].

The implications of the above analysis are that it should be possible to measure following chemical reaction rates *via* the SG–TC mode without any prior knowledge of the tip–substrate separation. From a practical viewpoint, this opens up the possibility of making such measurements with very basic positioning apparatus. The range of measurable rate constants will largely be governed by the timescale on which tip currents can be recorded. For example, towards the fast kinetic limit, a normalised peak current in excess of unity is predicted for $\log K = 2.5$, with tip–substrate separations closer than $\log(d/a) < -0.8$. The normalised time at which the peak occurs is, however, smaller than 0.01 . For a tip UME with a radius of $10 \mu\text{m}$ and a typical diffusion coefficient of $10^{-5} \text{ cm}^2 \text{ s}^{-1}$, these figures relate to a rate constant in excess of 3000 s^{-1} and a corresponding peak time less than 10^{-3} s . Under the experimental conditions of this study, with a large

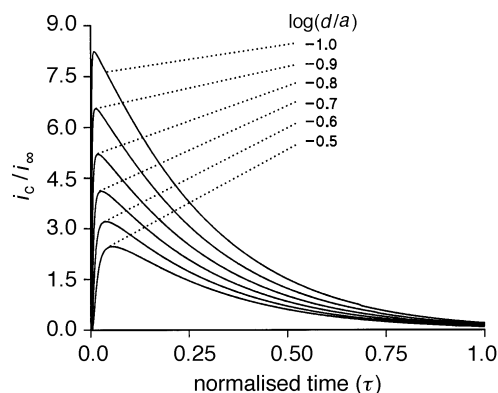


Fig. 3 Effect of tip–substrate separation on the SG–TC tip collector chronoamperometric response. The theoretical data relate to $K = 10$, with a range of defined $\log(d/a)$ values.

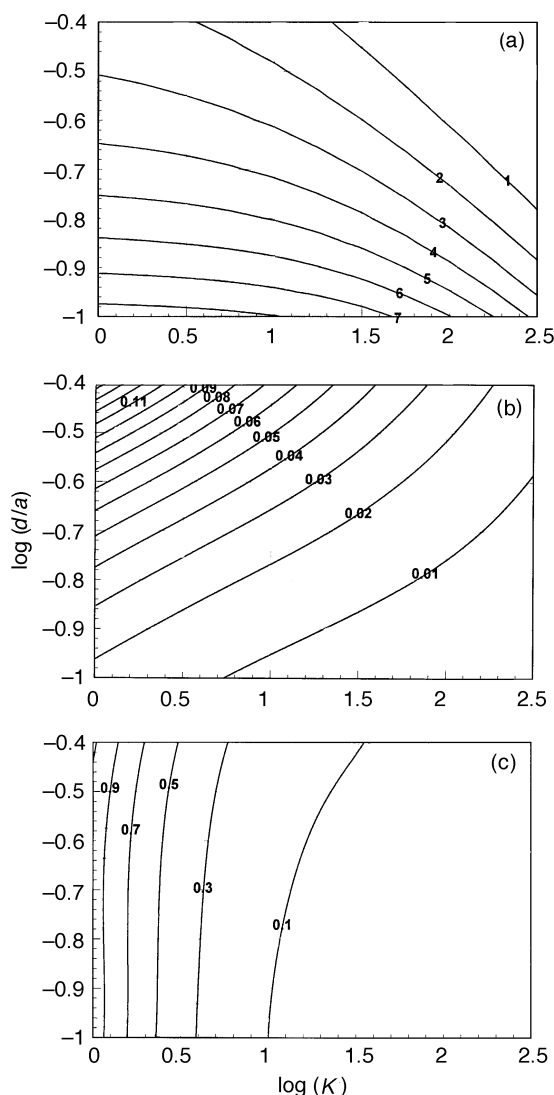


Fig. 4 Theoretical contour plots showing the variation of (a) peak current, (b) peak time and (c) post-half-peak time, with tip-substrate separation and normalised rate constant. The labels on the contours are either values of the normalised current ratio (a) or normalised time [(b) and (c)].

substrate electrode and conventional bipotentiostat, these parameters probably characterise the upper limit of rate constants that may be determined with the technique, since at shorter times there may be coupling between the substrate and tip responses.¹ By employing smaller substrate electrodes, it might be possible to push the SG-TC measurements to higher rate constants, comparable to those of $ca. 10^4 \text{ s}^{-1}$ attainable with the feedback mode.⁴

Experimental

Apparatus and instrumentation

Experiments were carried out in a four-electrode arrangement using an Oxford Electrodes (UK) bipotentiostat, which was modified in house to include an option which allowed currents to be measured with gains of 10^{-6} – 10^{-9} A V^{-1} , as well as the conventional 10^{-3} – 10^{-6} A V^{-1} range. Chronoamperometric characteristics were acquired directly on a NIC310 (Nicolet) digital storage oscilloscope with disk storage facilities.

A $25 \mu\text{m}$ diameter Pt disk UME, characterised by $RG = 10$, and prepared as described previously,^{15,16,19} was used as the tip electrode. The substrate electrode was a platinum (Goodfellow Metals, Cambridge, UK) square of area, $A = 4 \text{ mm}^2$, with a contact wire attached, potted flat in a cylinder of

epoxy resin (Delta Resins, Stockport, UK), and then ground to expose the Pt surface. Both the substrate and the tip electrode were polished with a succession (25, 14, 6 and $1 \mu\text{m}$) of finer diamond lapping compounds (Buehler Ltd, Coventry, UK) on nylon pads (Buehler) and finally using $0.05 \mu\text{m}$ alumina (Buehler). A platinum gauze was used as a counter-electrode and a silver wire served as a quasi-reference electrode (AgQRE).

The position of the UME tip was controlled by mounting it on a model 461 manual x – y – z stage (Newport Corp.). The z -axis was controlled by a differential micrometer (model DM-13, Newport Corp.) and the x and y axes by fine adjustment screws (Model AJS-05, Newport Corp.). The spatial resolution attainable with the micrometer was quoted as $0.07 \mu\text{m}$, but the device was used to measure the tip position to the nearest $0.25 \mu\text{m}$ (half of one division on the Vernier scale).

The cell comprised a fully detachable Teflon base, a cylindrical glass body and a Teflon lid. The base contained a hole in the centre that could securely accommodate the Pt substrate electrode, such that the surfaces of the substrate and tip electrodes were parallel. The stages and cell were mounted on a Newport CSD series breadboard which provided adequate vibration isolation.

Experiments involved placing the tip UME in contact with the substrate electrode and then withdrawing the tip a set distance from the substrate. There was effectively no positional offset with the set-up described. As found by other workers,¹⁴ the alignment between the tip and the substrate was sufficiently precise that when the two electrodes were placed together, electrical contact was made, as verified by the passage of a large anodic current with the substrate externally unbiased and the tip at a potential of 0.40 V vs. AgQRE to effect the oxidation of DMPPD.

Materials

DMPPD (Aldrich, Gillingham, UK) solutions ($4 \times 10^{-3} \text{ mol dm}^{-3}$) were prepared from a thoroughly deaerated $4 \times 10^{-2} \text{ mol dm}^{-3}$ stock solution immediately prior to each experiment using Milli-Q reagent water (Millipore Corp.), with 1.0 mol dm^{-3} potassium chloride (Fisons, AR grade) as a supporting electrolyte and 0.25 mol dm^{-3} dipotassium hydrogen phosphate (Fisons) as a buffer. The pH of the buffer was adjusted to the desired level with 1.0 mol dm^{-3} sodium hydroxide solution (Fisons).

Prior to all experiments, solutions were thoroughly deaerated with argon, for a period of $ca. 20 \text{ min}$. During experiments, Ar was passed over the surface of the solution under study. All measurements were made at $25 \pm 1^\circ\text{C}$.

Experimental results and discussion

The theoretical model assumes that the electrolysis of the solution precursor at the generator electrode is a simple diffusion-limited process, without any heterogeneous kinetic complications. Initial experiments were performed to demonstrate that this was the case for DMPPD oxidation in aqueous solution at pH 7.65, where the following chemical step [eqn. (V)] is negligible.⁴ These measurements were important since, although previous SECM feedback measurements have demonstrated that stable diffusion-limited currents are maintained for up to 15 min,⁴ provided that the concentration of DMPPD is low and the solution is thoroughly deaerated, there are also reports of filming of the electrode surface in studies carried out with conventional electrodes.²³

Potential-step chronoamperometric experiments were carried out by stepping the potential of the macroscopic generator electrode from 0.0 V , where there were no Faradaic processes to a value of 0.50 V , well into the limiting-current region, where the oxidation of DMPPD was driven at a

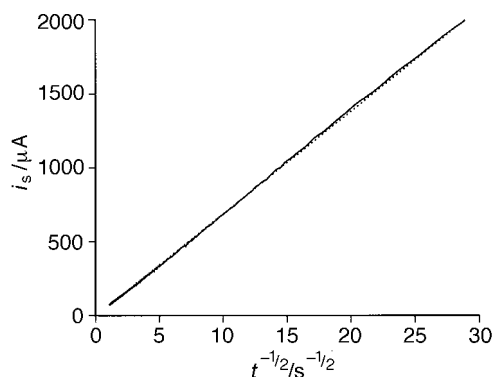


Fig. 5 Substrate (generator) electrode chronoamperometric response for the oxidation of DMPPD (—). The best fit of the experimental data to the behaviour predicted by eqn. (17), with $D = 7.2 \times 10^{-6} \text{ cm}^2 \text{ s}^{-1}$ is also shown (· · ·).

diffusion-controlled rate. Current transients were found to agree well with the Cottrell equation²⁷

$$i_s = \frac{nFAD^{1/2}c^*}{\pi^{1/2}t^{1/2}} \quad (17)$$

on a timescale of 0.5 ms and longer. In eqn. (17), c^* is the bulk concentration of DMPPD, i_s is the substrate electrode current and the other terms have been defined earlier. Eqn. (17) applied to experimental data obtained both without and with a tip located close (within micrometre distances) to the substrate electrode. Fig. 5 shows a typical chronoamperogram, plotted according to eqn. (17), for the generator electrode in a pH 7.65 solution with the UME tip positioned 5 μm above, and held at a potential of 0.0 V so as to collect the product of the substrate electrode reaction. The data yield a diffusion coefficient of $7.2(\pm 0.1) \times 10^{-6} \text{ cm}^2 \text{ s}^{-1}$ which is in good agreement with previously published results.⁴

The tip collector currents are sensitive to the ratio of diffusion coefficients of the reduced and oxidised forms of the couple, γ . Recent work from this group has demonstrated that SG-TC and feedback measurements in combination, represent a simple approach for determining this parameter. In particular, for a chemically stable couple, the ratio of the steady-state tip feedback current, i_f , and collector current, at close inter-electrode separations reveals γ directly.¹⁵

$$\gamma = i_c/i_f \quad (18)$$

without prior knowledge of the tip-substrate separation. Fig. 6 shows the feedback and SG-TC tip collector chronoamperometric responses at a tip-substrate separation of 5.0 μm . This distance was inferred, in this case, from the steady-state feedback current which is γ -independent.^{16,25} Feedback measurements were made by stepping the tip UME potential

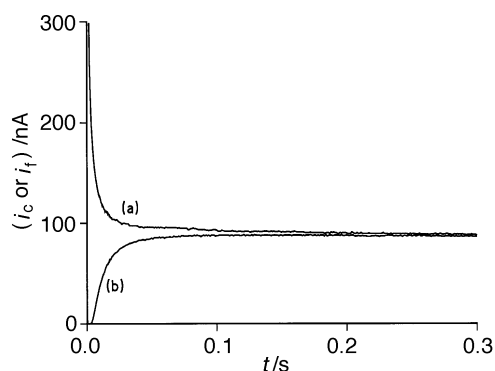


Fig. 6 (a) Feedback and (b) SG-TC tip collector chronoamperometric responses for DMPPD oxidation at pH 7.65 with a fixed tip-substrate separation of 5.0 μm . The transients reach similar steady-state values indicating that the ratio of diffusion coefficients (γ) of the electrode reactant and product is close to unity [eqn. (18)].

from 0.0 to 0.5 V to effect the diffusion-controlled oxidation of DMPPD, with the substrate potential maintained at 0.0 V to drive the reverse process at diffusion control. For the SG-TC measurements, the applied potentials were interchanged. The steady-state responses are seen to be very close at long times, yielding a value of $\gamma = 0.98 (\pm 0.02)$. This indicates that the diffusion coefficients of the reduced and oxidised forms of DMPPD are very close, and may be considered to be effectively equal, within experimental error.

Fig. 7 shows the SG-TC tip collector transients, recorded as described above, at several other tip-substrate separations, at pH 7.65. Also shown are the corresponding theoretical predictions for the case of $K = 0$, for each of the inter-electrode separations of interest. The experimental characteristics are consistent with the predictions above [Fig. 2(a) and (b)] showing clearly that the product of the electrode reaction [eqn. (IV)] is effectively stable on the timescale of SECM measurements at the defined pH.

A selection of typical tip current responses are shown in Fig. 8 for the oxidation of DMPPD at the substrate electrode and collection of the generator product [eqn. (IV)] at the tip, with the solution at three higher pH values (10.94, 11.36 and 11.54) to promote the deamination process [eqn. (V)]. The potentials applied to the substrate and tip electrodes were as defined above for SG-TC measurements. The shapes of the tip transients are consistent with the theoretical predictions for an EC process, with the collector current initially rising to a peak value and then decaying at longer times. The best fits of the model to each of the transients are also shown for comparison with experiment. In each case, the inter-electrode separation and diffusion coefficient of DMPPD was known and thus the rate constant, k_c , was the only variable in the fitting procedure. There is seen to be reasonable agreement between experiment and theory. Moreover, the transients at different pH yield a consistent rate constant for the deamination step, with values of k_c of 8.8 s^{-1} [(a), pH 10.94], 23 s^{-1} [(b), pH 11.36] and 33 s^{-1} [(c) pH 11.54]. For comparative purposes, approximating the measured activity by concentration of OH^- , these values yield a second-order rate constant, $k_2 = k_c/[\text{OH}^-] = 1.0(\pm 0.1) \times 10^4 \text{ mol}^{-1} \text{ dm}^3 \text{ s}^{-1}$, in good agreement with previously published results for this system (with the same approximation) obtained with the SECM feedback mode.⁴

It is useful, finally, to examine practically the precision with which the SG-TC methodology can determine both the rate constant and inter-electrode separation. Fig. 9 shows the sets of inter-electrode spacings and rate constants derived from the peak currents and peak times of the transients in Fig. 8. The intersection of the two contours on each plot yields the following values of d and k_c : (a) 2.7 μm and 9.2 s^{-1} (pH 10.94); (b) 1.9 μm and 30 s^{-1} (pH 11.36) and (c) 2.6 μm and 37 s^{-1}

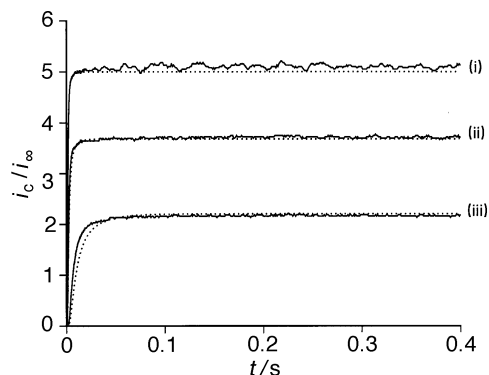


Fig. 7 Tip (collector) electrode chronoamperometric responses for the oxidation of DMPPD (—) at pH 7.65 in the SG-TC mode, with tip-substrate separations of (i) 1.25, (ii) 2.25 and (iii) 3.25 μm . The corresponding theoretical responses for these distances with $K = 0$ are shown for comparison (· · ·).

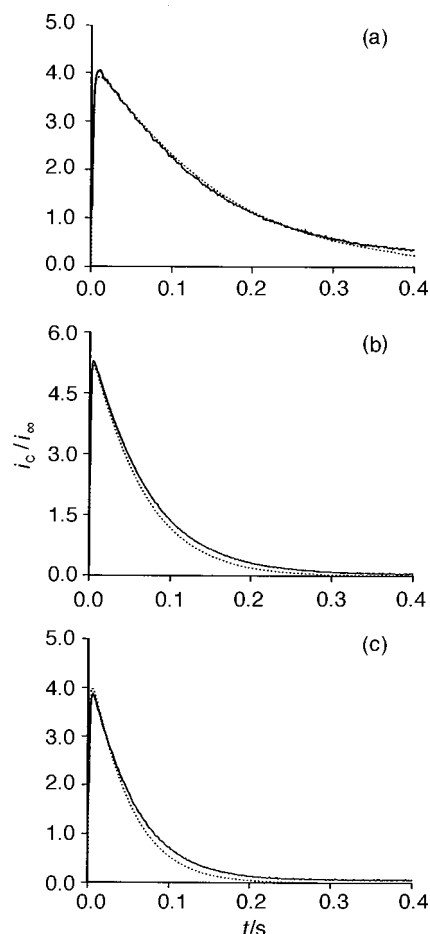


Fig. 8 Tip (collector) electrode chronoamperometric responses for the oxidation of DMPPD (—) under the following conditions: (a) pH 10.94, $d = 2.75 \mu\text{m}$; (b) pH 11.36, $d = 2.0 \mu\text{m}$; (c) pH 11.54, $d = 2.5 \mu\text{m}$. The experimental data have been fitted to theory (\cdots) using the value of D cited in the text and k_c : (a) 8.8; (b) 23; (c) 33 s^{-1} .

(pH 11.54). The values of inter-electrode separation are close to those expected, while the rate constants are in good agreement with those used in fitting the full tip transients (see the caption to Fig. 8). The set of rate constants derived from surface fitting the peak currents and times yields $k_2 = 1.15 (\pm 0.15) \times 10^4 \text{ mol}^{-1} \text{ dm}^3 \text{ s}^{-1}$. The results of this exercise thus clearly show that the rate constants for following chemical reactions and inter-electrode separations can be determined with good precision and accuracy from the measurement of the peak current and peak time from tip collector transient measurements in the SG-TC mode.

Conclusions

The first theoretical model for the SG-TC mode with EC processes has been developed and shown to be in excellent agreement with experimental measurements on the oxidation of DMPPD in aqueous solution at high pH. The theory advances an earlier model¹² by taking full account of feedback effects which are shown to be important. If the inter-electrode separation is known, the SG-TC mode can be used to measure following chemical reaction rates by fitting the full tip current transient response, with the homogeneous rate constant as the only variable. Alternatively, both the rate constant and inter-electrode separation can be determined with high precision by simply measuring the peak current and peak time in a single transient. This latter approach negates the need for sophisticated positioning apparatus for SECM measurements of this type.

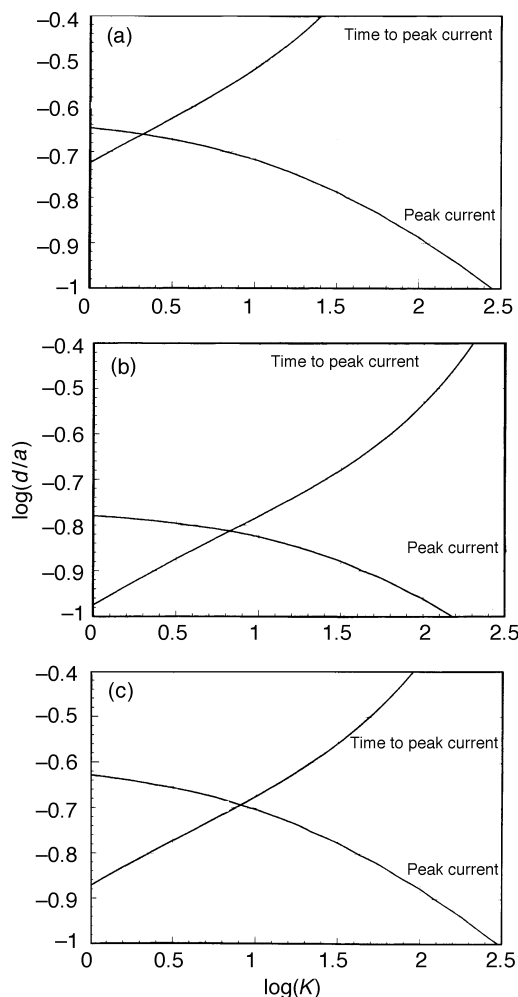


Fig. 9 Contours showing the sets of values of $\log(d/a)$ and $\log K$ derived from measurements of the peak current and peak time from the transients in Fig. 8. Data relate to the measurements at pH: (a) 10.94, (b) 11.36 and (c) 11.54.

The upper limit to the rate constants measurable with the technique is close to that of the feedback mode⁴ and could surpass it with improvements in the electrochemical instrumentation employed. From a practical viewpoint, the technique is unlikely to match the TG-SC mode operating with two closely spaced UMEs.^{5,6} The latter approach does, however, require high-precision positioning capabilities of the tip and collector electrodes in all three spatial coordinates. The SG-TC methodology could readily be extended to other classes of coupled chemical processes, such as second-order following chemical reactions, sandwiched solution processes (as in the ECE-DISP scheme) or parallel (catalytic) solution reactions.

We thank the EPSRC for a studentship for R. D. M. Helpful discussions on this work with Dr Julie Macpherson (University of Warwick) are much appreciated.

References

- 1 A. J. Bard, F. R. F. Fan, J. Kwak and O. Lev, *Anal. Chem.*, 1989, **61**, 132.
- 2 A. J. Bard, F. R. F. Fan, D. T. Pierce, P. R. Unwin, D. O. Wipf and F. Zhou, *Science*, 1991, **254**, 68.
- 3 For recent reviews see *e.g.* (a) A. J. Bard, M. V. Mirkin and F. R. F. Fan, in *Electroanalytical Chemistry*, ed. A. J. Bard, Marcel Dekker, New York, 1993, vol. 18, p. 243; (b) M. Arca, A. J. Bard, B. R. Horrocks, T. C. Richards and D. A. Treichel, *Analyst*, 1994, **119**, 719; (c) J. V. Macpherson and P. R. Unwin, *Chem. Ind.*, 1995, 874; (d) M. V. Mirkin, *Anal. Chem.*, 1996, **68**, 177A.
- 4 P. R. Unwin and A. J. Bard, *J. Phys. Chem.*, 1991, **95**, 7814.

- 5 F. Zhou, P. R. Unwin and A. J. Bard, *J. Phys. Chem.*, 1992, **96**, 4917.
- 6 C. Demaille, P. R. Unwin and A. J. Bard, *J. Phys. Chem.*, 1996, **100**, 14137.
- 7 T. C. Richards, A. J. Bard, A. Cusanelli and D. Sutton, *Organometallics*, 1994, **13**, 757.
- 8 D. A. Treichel, M. V. Mirkin and A. J. Bard, *J. Phys. Chem.*, 1994, **98**, 5751.
- 9 F. Zhou and A. J. Bard, *J. Am. Chem. Soc.*, 1994, **116**, 393.
- 10 C. Lee, J. Kwak and F. C. Anson, *Anal. Chem.*, 1991, **63**, 1501.
- 11 C. Wei, A. J. Bard, G. Nagy and K. Toth, *Anal. Chem.*, 1995, **67**, 1346.
- 12 R. C. Engstrom, M. Weber, D. J. Wunder, R. Burgess and S. Winquist, *Anal. Chem.*, 1986, **58**, 844.
- 13 R. C. Engstrom, T. Meaney, R. Tople and R. M. Wightman, *Anal. Chem.*, 1987, **59**, 2005.
- 14 M. V. Mirkin, H. Yang and A. J. Bard, *J. Electrochem. Soc.*, 1992, **139**, 2212.
- 15 R. D. Martin and P. R. Unwin, *Anal. Chem.*, 1998, **70**, 276.
- 16 R. D. Martin and P. R. Unwin, *J. Electroanal. Chem.*, 1997, **439**, 123.
- 17 D. W. Peaceman and H. H. Rachford, *J. Soc. Ind. Appl. Math.*, 1955, **3**, 28.
- 18 L. Lapidus and G. F. Pinder, *Numerical Solutions of Partial Differential Equations*, Wiley, New York, 1977.
- 19 See e.g. (a) P. R. Unwin and A. J. Bard, *J. Phys. Chem.*, 1992, **96**, 5035; (b) D. T. Pierce, P. R. Unwin and A. J. Bard, *Anal. Chem.*, 1992, **64**, 1795; (c) J. V. Macpherson and P. R. Unwin, *J. Phys. Chem.*, 1994, **98**, 1704; (d) J. V. Macpherson and P. R. Unwin, *J. Phys. Chem.*, 1994, **98**, 11764; (e) J. V. Macpherson and P. R. Unwin, *J. Phys. Chem.*, 1995, **99**, 3338; (f) J. V. Macpherson and P. R. Unwin, *J. Phys. Chem.*, 1995, **99**, 14824; (g) J. V. Macpherson and P. R. Unwin, *J. Phys. Chem.*, 1996, **100**, 19475; (h) J. V. Macpherson, C. J. Slevin and P. R. Unwin, *J. Chem. Soc., Faraday Trans.*, 1996, **92**, 3799; (i) J. V. Macpherson, D. O'Hare, P. R. Unwin and C. P. Winlove, *Biophys. J.*, 1997, **73**, 2771.
- 20 C. J. Slevin, J. V. Macpherson and P. R. Unwin, *J. Phys. Chem. B*, 1997, **101**, 10851.
- 21 A. L. Barker, J. V. Macpherson, C. J. Slevin and P. R. Unwin, *J. Phys. Chem. B*, in press.
- 22 L. K. J. Tong, *J. Phys. Chem.*, 1954, **58**, 1090.
- 23 L. K. J. Tong, K. Liang and W. R. Ruby, *J. Electroanal. Chem.*, 1967, **13**, 245.
- 24 K. Aoki and H. Matsuda, *J. Electroanal. Chem.*, 1978, **94**, 157.
- 25 J. Kwak and A. J. Bard, *Anal. Chem.*, 1989, **61**, 1221.
- 26 Y. Saito, *Rev. Polarogr. Jpn.*, 1968, **15**, 177.
- 27 A. J. Bard and L. R. Faulkner, *Electrochemical Methods*, Wiley, New York, 1980.

Paper 7/07984B; Received 5th November, 1997